

The validation and application of a Super-resolution PIV Post-Processing Method Based on Sub-Pixel Image Shifting and Optical Flow

Peidong Tian¹, Fang Chen^{1*}

¹ Shanghai Jiao Tong University / School of Aeronautics and Astronautics/Shanghai, China

* fangchen@sjtu.edu.cn

Abstract

A super-resolution PIV post-processing method based on sub-pixel image shifting and optical flow method is proposed. The overall accuracy of the PIV result is improved without obtaining other information, and the super-resolution result is obtained. This method can provide more small-scale flow structure information for the study of combustion, shock and vortex.

A new image shifting method is proposed, which allows pixels to shift to the interval of the pixel grid, reconstruct the image without losing the displacement information due to rounding, and make the new post-processing method suitable for any type of PIV algorithm.

According to the validation result of the synthetic PIV image, the root mean square (rms) error obtained by the post-processing method is significantly smaller than that of the original PIV result. A set of experimental images is analyzed. The results show that the super-resolution PIV post-processing method can reduce the influence of image defects on the displacement field calculation, in addition to obtaining higher displacement field accuracy.

1 Introduction

For 2-D PIV technique, the accuracy, resolution and dynamic range are the most concerned aspects to be improved as is mentioned by Kähler et al. (2016) in the results of the 4th international PIV challenge.

The resolution is firmly depended on the size of the interrogation window, so several methods have been introduced to increase the resolution by decreasing the interrogation window size. Multiple Pass Interrogation is commonly used to decrease the interrogation window size by offsetting the interrogation windows according to the mean displacement. Grid Refining Schemes, a further improved multiple pass method, can narrow down the interrogation window to the size smaller than the particle image displacement. For flow with significant velocity gradients, Iterative Image Deformation method introduced by Scarano (2002) is implemented into the multi-grid method to get adaptive spatial resolution, increasing the accuracy in general.

Another approach to increase spatial resolution so-called Super Resolution PIV is suggested and evaluated by Hart (2000) and F Billy et al. (2004) Super-Resolution PIV obtains a resolution of one vector per pixel, but it requires a series of image pairs for iteration which limits its utilization.

A hybrid method combining cross-correlation and optical flow method has been firstly implemented by Yang et al. (2016) to improve the PIV accuracy. The hybrid method shifts image based on estimate displacement field to form a reconstructed image, and analyze the reconstructed image with the corresponding actual image by optical flow method to fix the estimate velocity field. The hybrid method gives super-resolution result while improving PIV accuracy. The image shift method has been

applied to recent research as a PIV uncertainty quantification approach by Sciacchitano A et al. (2013) and Wieneke B (2015), proving to be valid.

Based on Yang's algorithm, a post-processing method is present. Assume there is a PIV image pair, image A and image B, and a rough displacement field has been found through cross-correlation method. This post-processing method fills the displacement field by interpolation, and shifts the pixels of image A according to the filled displacement field, and obtains a reconstructed new image B', which will be slightly different with image B. The formed image B' is compared with image B, with their difference calculated by optical flow method to modify the previous displacement field. This post-processing method can be easily implanted to any PIV processing program based on the cross-correlation algorithm, and its output improves the accuracy and expands the spatial resolution to pixel level at the same time.

In order to improve the accuracy of the image, a new image shifting algorithm is proposed. The original method is limited to displacements that are integer multiples of the pixel size. The improved method can handle non-integer displacement fields. Therefore, it can be applied to sub-pixel interpolation PIV results. Compared with the original method, the new method is more accurate, especially in low-resolution images.

2 Super-resolution PIV Post Processing Method

The Super-resolution PIV Post Processing Method is a post-process based on optical flow method to enhance the results of standard cross-correlation PIV methods, or any other PIV image process method. The algorithm contains three main parts: displacement field interpretation, pixel shift, and optical flow method process; all will be explained in detail in the following parts.

Define the image pair as image A(The first image) and image B(The second picture). A sparse displacement field is presented by cross-correlation result of image A and image B. Then the displacement field is filled through linear interpolation. Based on the full filled displacement field, each pixel of image A is shifted to form a new image, which has a similar pattern as image B because the pixels are shifted based on the estimate motion of real particles. The new image is called reconstructed image B'. Optical flow method is implemented on image B' and image B to get a displacement field reflecting the difference between the estimate particle motion with the real particle motion. The two displacement fields are combined to form the final result with relatively high accuracy and pixel level resolution. The whole process is shown in Fig. 1.

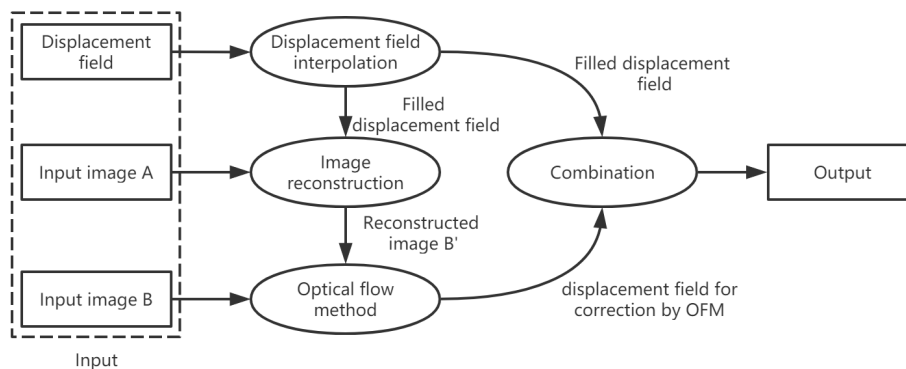


Figure 1: Flow chart of the post-processing method

2.1 Cross-correlation and post-processing

Cross-correlation over a pair of images is a statistical approach, selecting and matching small image areas (interrogation window) to find the corresponding particle displacement. For each interrogation window selected in image A, a set of interrogation windows are selected in image B. To find the most

probable interrogation window in image B matching with the interrogation window in image A; the discrete cross-correlation function is implemented:

$$C_{II}(x, y) = \sum_{i=0}^M \sum_{j=0}^N [I(i, j) - \mu_I][I'(i + x, j + y) - \mu_{I'}(x, y)] \quad (1)$$

$$\sigma_I(x, y) = \sum_{i=0}^M \sum_{j=0}^N [I(i, j) - \mu_I]^2 \quad (2)$$

$$\sigma_{I'}(x, y) = \sum_{i=0}^M \sum_{j=0}^N [I'(i, j) - \mu_{I'}(x, y)]^2 \quad (3)$$

$$C_{ii}(x, y) = \frac{C_{II}(x, y)}{\sqrt{\sigma_I(x, y)}\sqrt{\sigma_{I'}(x, y)}} \quad (4)$$

Where $C_{ii}(x, y)$ is the normalized discrete cross-correlation coefficient. To get sub-pixel precision particle displacement, The correlation peak should be estimated to sub-pixel accuracy. Implement the most common Gaussian peak fit as three-point estimator as follow:

$$x_0 = i + \frac{\ln C(i-1, j) - \ln C(i+1, j)}{2 \ln C(i-1, j) - 4 \ln C(i, j) + 2 \ln C(i+1, j)} \quad (5)$$

$$y_0 = j + \frac{\ln C(i, j-1) - \ln C(i, j+1)}{2 \ln C(i, j-1) - 4 \ln C(i, j) + 2 \ln C(i, j+1)} \quad (6)$$

Here x_0 and y_0 are the coordinate of the estimated correlation peak. i and j are the coordinate of the maximum value point of the correlation plane C_{ii} .

To obtain reliable displacement matrix, data validation and correction is needed. Two widely used data validation methods are Global Histogram Operator and Normalized Median Test. Through the post-processing above, the false data are recognized and replaced. The replacement of the missing data uses whether bilinear interpolation or weighted average of the surrounding data.

2.2 Velocity filling

The displacement obtained from cross-correlation covers only the point on the center of corresponding interrogation windows. In order to form a complete displacement field which contains the displacement vector for every pixel, displacement vectors on other points remain to be filled. Every empty point is therefore interpolated with a displacement vector linearly.

2.3 image shift

To form a reconstructed image B' to compare with actual image B, each pixel in image A is shifted according to the estimated displacement field.

The principle is that each particle remains the same intensity on image A and image B. Consider each pixel in image A as a single luminous particle, and displace it according to the displacement field. The particle will fall into a point surrounded by 4 pixels, and its intensity is separated and add to these 4 pixels. The accumulation of all the displaced pixel forms the reconstructed image B' . The algorithm is operated as follow:

For every pixel $A_{(i,j)}$ in image A, and $Q_{i,j}$ is the impact matrix indicate the intensity contribution of the pixel on the point (i, j) in image A after shift, as is showed in Fig. 2(a). It is defined as:

$$Q_{i,j(m,n)} = \delta(1 - |i' - m|)(1 - |j' - n|)A_{(i,j)} \quad (7)$$

where, i' and j' are the coordinate of the pixel after shift.

$$i' = i + u_{(i,j)} \quad (8)$$

$$j' = j + v_{(i,j)} \quad (9)$$

Here $u_{(i,j)}$ and $v_{(i,j)}$ is respectively the component of the displacement vector in i direction and j direction.

δ is a factor that equal to 1 only when the point (m, n) is the four surrounding integer points of (i', j') :

$$\delta = \begin{cases} 1, & |i' - m| < 1 \text{ and } |j' - n| < 1 \\ 0, & \text{otherwise} \end{cases} \quad (10)$$

Accumulate impact matrix $Q_{i,j}$ of all pixels in image A results in matrix B' , which is the reconstructed image B' , as shown in Fig. 2(b)

$$B' = \sum_i \sum_j Q_{(i,j)} \quad (11)$$

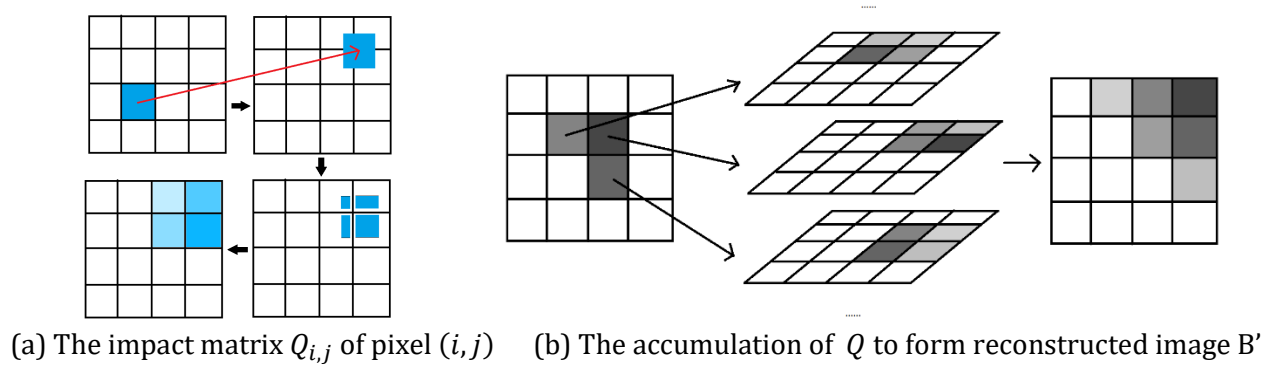


Figure 2: Two test figures. Please try to match the font sizes in the figures with the text.

2.4 optical flow method

Optical Flow method by Farneback(2003) is a two-frame motion estimation algorithm. For each pixel, a quadratic polynomial expansion expressed in a local coordinate system is estimated to approximate its neighborhood as

$$f(x) \sim x^T R x + b^T x + c \quad (12)$$

Symmetric matrix R , vector b and scalar c are estimated from a weighted least squares fit to the signal values in the neighborhood. $f(x)$ is the intensity distribution matrix in a certain field.

A displacement d acting on results in the polynomial below

$$\begin{aligned} f_2(x) &= f_1(x - d) \\ &= (x - d)^T R_1 (x - d) + b_1^T (x - d) + c_1 \\ &= x^T R_1 x + (b_1 - 2R_1 d)^T x + d^T R_1 d - b_1^T d + c_1 \\ &= x^T R_2 x + b_2^T x + c_2 \end{aligned} \quad (13)$$

So d can be solved by

$$d = -\frac{1}{2} R_1^{-1} (b_2 - b_1) \quad (14)$$

We get the polynomial expansion $R_1(x)$, $b_1(x)$, $c_1(x)$ for image B' and $R_2(x)$, $b_2(x)$, $c_2(x)$ for image B . The expansion coefficients is averaged as

$$R(x) = \frac{R_1(x)+R_2(x)}{2} \quad (15)$$

And introduce $\Delta b(x)$

$$\Delta b(x) = -\frac{1}{2}(b_2(x) - b_1(x)) \quad (16)$$

Then the displacement $d(x)$ can be solved by

$$R(x)d(x) = \Delta b(x) \quad (17)$$

Pyramid method is implied to enlarge the detect range. An image pyramid is generated with different resolution levels. Downsampling the previous level generates each pyramid level. Starting from the lowest resolution, estimate the displacement field. At each level, the result from the previous level is used as an initial guess of the displacement field. The displacement will be refined until the original image is analyzed. With the pyramid method, displacement more significant than the neighborhood size can be detected.

3 result and discussion

3.1 validation on synthetic PIV image

The velocity fields of the synthetic PIV image pair are set as typical shear flow field $u = K \tanh(\beta y)$. The parameters in table 1 are used to generate the image pair. Here case S is set as the standard group. The generated image of S is shown as Fig.3. Group A is set to find the impact of out-of-plane motion condition on the result. Group B and group C is used to compare the impact of different particle number and particle size, respectively. The density and size are chosen based on the discussion of particle tracking characteristics by Chen F et al. (2017) PIV particle image is generated according to the principle proposed by Okamoto et al. (2000)

Table 1: Synthetic PIV image generation conditions of different test groups

CASE	image size	sheet thickness	Umax	particle size	Nr. of particle	out-of-plane motion
S	1000*1000	0.5	10	5	250000	0.015
A1	1000*1000	0.5	10	5	250000	0.005
A2	1000*1000	0.5	10	5	250000	0.01
A3	1000*1000	0.5	10	5	250000	0.015
A4	1000*1000	0.5	10	5	250000	0.02
A5	1000*1000	0.5	10	5	250000	0.025
B1	1000*1000	0.5	10	5	100000	0.015
B2	1000*1000	0.5	10	5	200000	0.015
B3	1000*1000	0.5	10	5	300000	0.015
B4	1000*1000	0.5	10	5	400000	0.015
C1	1000*1000	0.5	10	2	250000	0.015
C2	1000*1000	0.5	10	3	250000	0.015
C3	1000*1000	0.5	10	4	250000	0.015
C4	1000*1000	0.5	10	6	250000	0.015
C4	1000*1000	0.5	10	6	250000	0.015

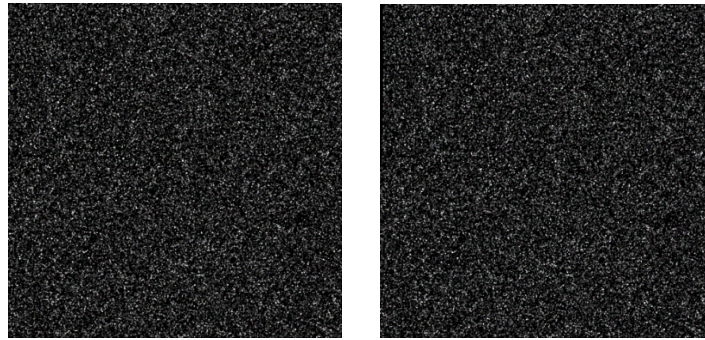


Figure 3: Synthetic PIV image of shear flow, standard group

The cross-correlation method and Farneback optical flow method were used to calculate the displacement vectors of the reference group images, respectively, and the super-resolution PIV post-processing method was applied then. The optical flow method uses the multi-resolution algorithm to calculate massive displacement. The cross-correlation algorithm uses FFT multi-grid method, using 64×64 , 32×32 , 16×16 triple grids to obtain data with smaller errors.

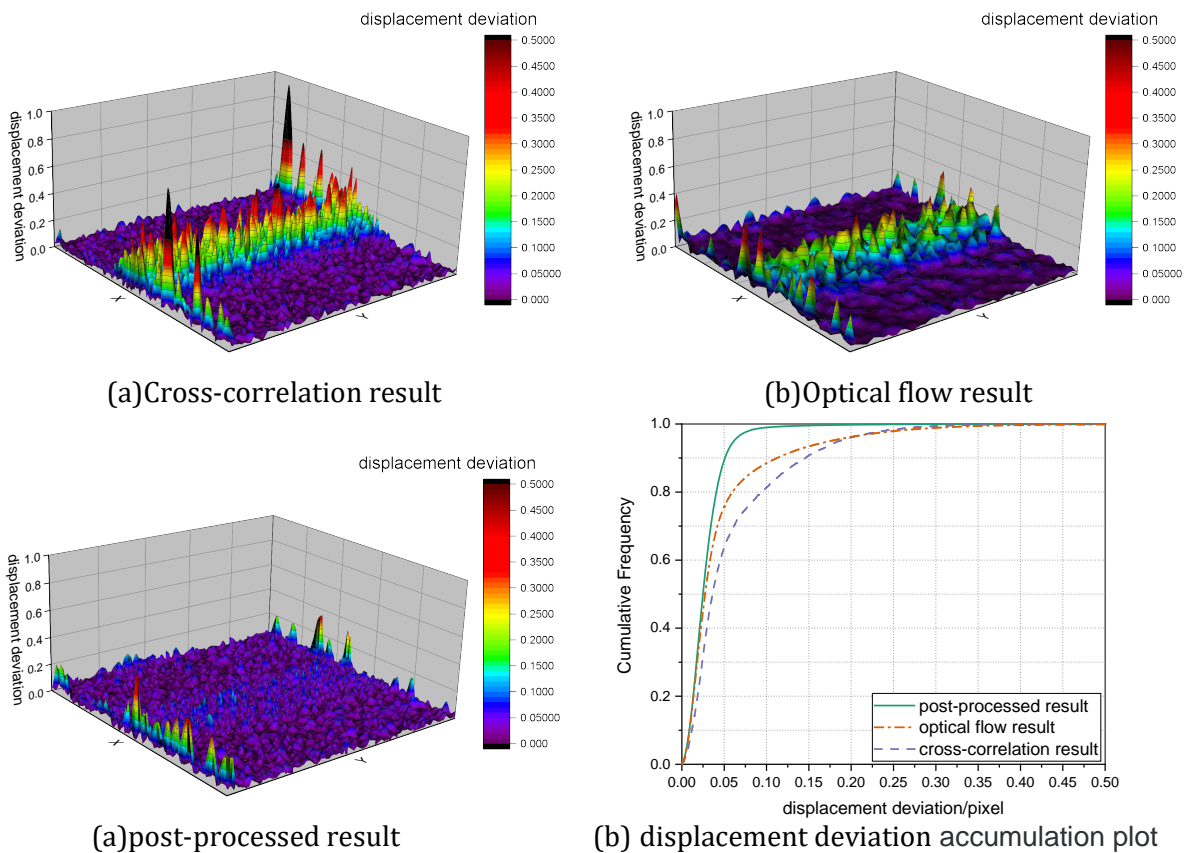


Figure 4: standard group analysis result. The displacement deviation indicates the difference of calculated displacement magnitude with the displacement magnitude of the synthetic image

In the standard case, the displacement deviations distribution obtained by the three methods are shown in Fig. 4 (a),(b) and (c). The RMS of the optical flow method, cross-correlation method, and cross-correlation method after post-processing is 0.0787, 0.0852, and 0.0376, respectively. It can be

seen from the RMS that the error of the post-processed result is the smallest. As can be seen from the displacement deviations distribution, where the velocity gradient in the middle region is large, both the optical flow method and the cross-correlation method have significant errors. Due to the large velocity gradient in this region, the optical flow method using multi-resolution algorithm will get wrong results at the lower resolution scale. Thus, the interpretation at the next scale level cannot be right, and the whole iteration process fails. The iterative cross-correlation algorithm of mesh deformation can obtain relatively accurate results to a certain extent. However, due to the limitation of mesh size, the final results obtained in the region with a large velocity gradient are superior to the optical flow method, but still, have a significant error. Meanwhile, the cross-correlation method cannot obtain the super-resolution displacement field. The super-resolution PIV post-processing method reconstructs the image based on the displacement field obtained by the cross-correlation method and modifies the image through the optical flow method. This operation can avoid the defect that the multi-resolution algorithm cannot deform the mesh, and gives play to the high accuracy of the optical flow method in the displacement calculation in a small range, and obtains better results than the cross-correlation algorithm and the optical flow method. For the boundary, the super-resolution PIV post-processing method cannot eliminate the boundary error, but can significantly reduce the boundary error. The reason for the super-resolution PIV post-processing method is that the estimation of massive displacement by the iterative mesh deformation cross-correlation algorithm is significantly better than that by the multi-resolution optical flow method. The super-resolution PIV post-processing method outperforms the two conventional methods in this case is because the estimation of massive displacement by iterative mesh deformation cross-correlation algorithm is significantly better than that by multiresolution optical flow method.

From the displacement deviation accumulation line, Fig.4(d), we find that 90% of the displacement deviation of the optical flow method results are within 0.1 pixels, and for the cross-correlation method, there is only 80%. Meanwhile, 99% of the displacement deviation of the post-processed results are within 0.1 pixels.

In order to show the influence of different factors on the performance of the three methods, the applicability of the methods is judged by the root-mean-square errors under different conditions. The results are shown in Fig. 5

The results show that the super-resolution post-process method outperformed others when dealing with images with a density of 0.2-0.3 particle per pixel.

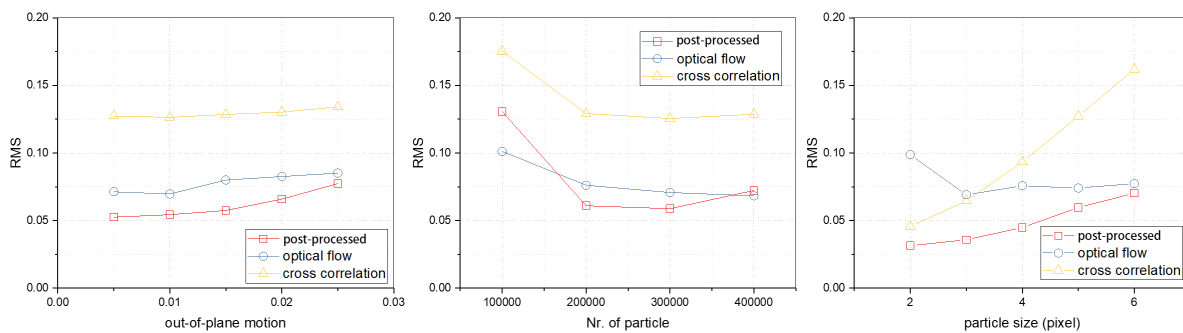


Figure 5: RMS of three methods apply to synthetic PIV image, corresponding to group A, group B, and group C, respectively

3.2 application of super-resolution PIV post-processing method in practical PIV experiments

Figure 6 shows a PIV image used to study the flow field of a flapping wing. In general, the displacement field obtained by the cross-correlation method has a large defect, and the calculation of the vortex center flow field is ineffective due to imaging defects. This defect can lead to the failure of the

correlation peak estimate in the cross-correlation algorithm. At the same time, the displacement field detects the vortex validly after the correction of the super-resolution post-processing method.

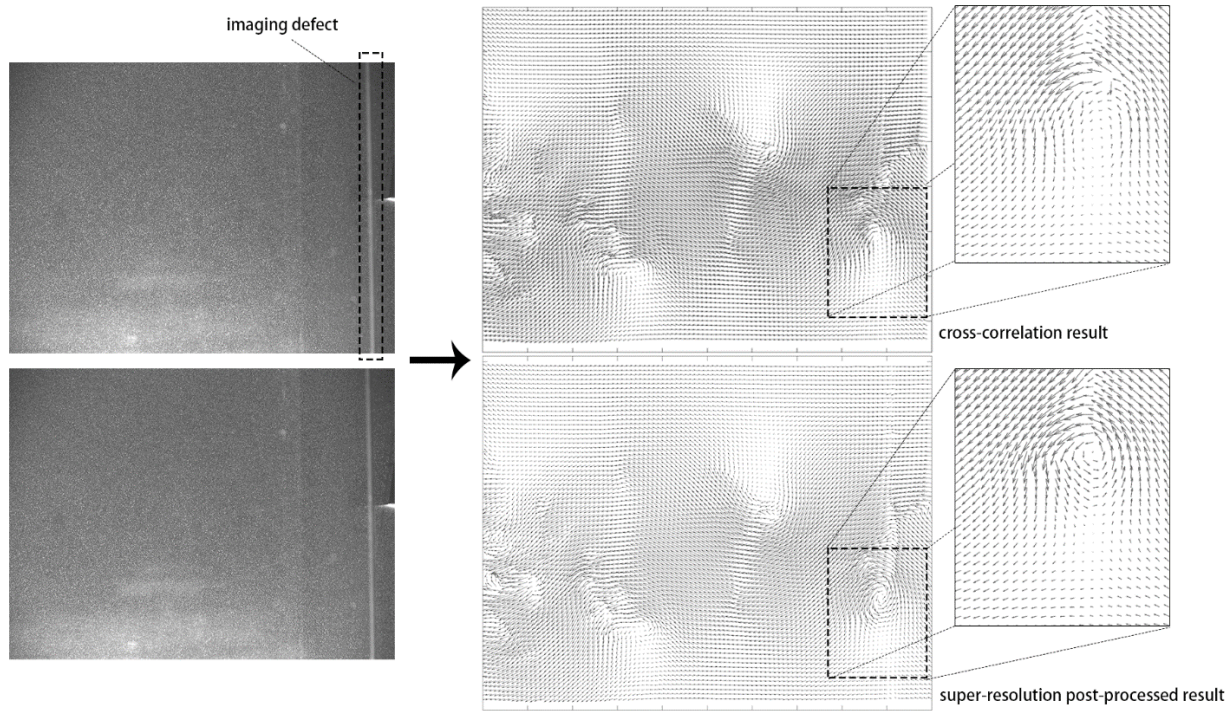


Figure 5: PIV image of a flow field behind a flapping wing being analyzed through cross-correlation method and super-resolution post process. The bright band at the right side of the image is a fixed imaging defect. The magnified area of the displacement field is a vortex located on the imaging defect band position

4 Conclusion

With the new sub-pixel image shifting method, the super-resolution PIV post-processing method can be adapted to the image analysis process regardless of the algorithm used to generate the initial displacement field. The integrated PIV image validation shows that the super-resolution PIV post-processing method is superior to the existing cross-correlation method in accuracy and resolution. The method is applied to the actual PIV experimental image, and the effectiveness and practicability of the method are verified. The effect of imaging defects is compensated to some extent, and a more reliable displacement field is obtained.

Acknowledgements

The authors gratefully acknowledge the financial support of the National Natural Science Foundation of China (No. 11672183 and 91641129)

References

- Kähler CJ, Astarita T, Vlachos PP, Sakakibara J, Hain R, Discetti S, La Foy R, and Cierpka C (2016) Main results of the 4th International PIV Challenge. *Experiments in Fluids* 57:97
- Scarano F (2002) Iterative image deformation methods in PIV. *Meas. Sci. Technol.* 13 R1

13th International Symposium on Particle Image Velocimetry – ISPIV 2019
Munich, Germany, July 22-24, 2019

Raffel M, Willert CE, Scarano F, Kähler CJ, Wereley ST, and Kompenhans J (2018) Particle Image Velocimetry. Chapter Image Evaluation Methods for PIV, page 145. Springer. 3rd edition

Tropea C, Foss JF, Yarin A (2007) Springer Handbook of Experimental Fluid Mechanics. Chapter Data Analysis, page 1437. Springer

Hart DP (2000) Super-Resolution PIV by Recursive Local-Correlation. *Journal of Visualization* 3:187

F Billy, L David, and G Pineau (2004) Single pixel resolution correlation applied to unsteady flow measurements. *Meas. Sci. Technol.* 15:1039

Yang Z, Johnson MJ (2017) Hybrid particle image velocimetry with the combination of cross-correlation and optical flow method. *Journal of Visualization* 20: 625

Sciacchitano A, Wieneke B, and Scarano F (2013) PIV uncertainty quantification by image matching. *Meas. Sci. Technol.* 24

Wieneke B (2015) PIV uncertainty quantification from correlation statistics. *Meas. Sci. Technol.* 26

Farneback G (2003) Two-Frame Motion Estimation Based on Polynomial Expansion. In *Scandinavian Conference on Image Analysis-SCIA2013 Espoo, Finland, June 17-20*

Chen F, Liu H, Yang Z, and Hu H (2017) Tracking characteristics of tracer particles for PIV measurements in supersonic flows. *Chinese Journal of Aeronautics* 30:577

Okamoto K, Nishio S, Saga T, and Kobayashi T (2000) Standard images for particle-image velocimetry. *Meas. Sci. Technol.* 11:685